Expanded Interactome of the Intrinsically Disordered Protein Dss1

Schenstrøm, Signe Marie; Rebula, Caio A.; Tatham, Michael H.; Hendus-Altenburger, Ruth; Jourdain, Isabelle; Hay, Ronald T.; Kragelund, Birthe B.; Hartmann-Petersen, Rasmus

Published in:
Cell Reports

DOI:
10.1016/j.celrep.2018.09.080

Publication date:
2018

Document version
Publisher's PDF, also known as Version of record

Report

Cell Reports

Expanded Interactome of the Intrinsically Disordered Protein Dss1

Graphical Abstract

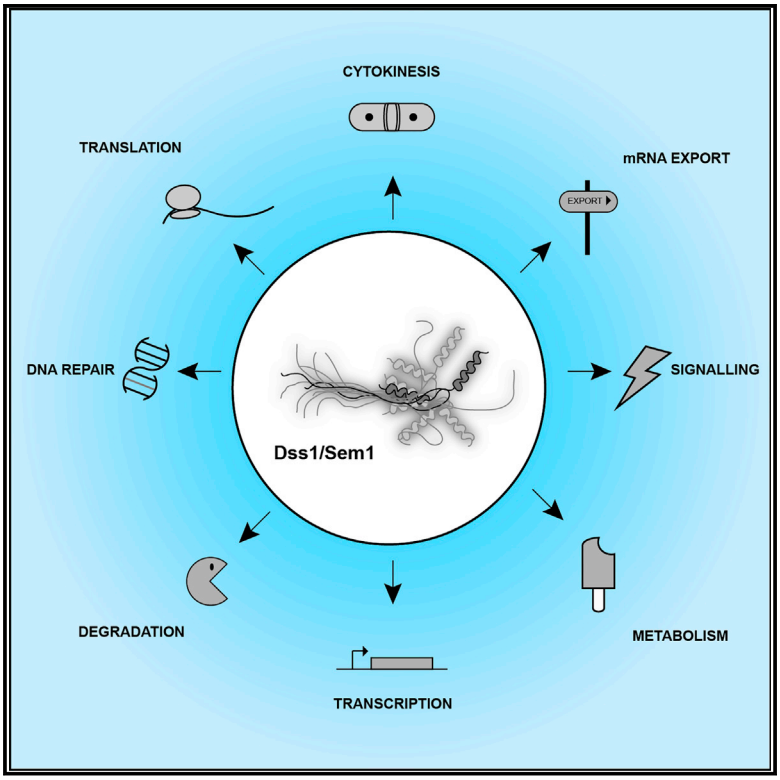

Authors

Signe M. Schenstrøm, Caio A. Rebula, Michael H. Tatham, ..., Ronald T. Hay, Birthe B. Kragelund, Rasmus Hartmann-Petersen

Correspondence

rhpetersen@bio.ku.dk

In Brief

Schenstrøm et al. demonstrate that the disordered protein Dss1 forms a transient intramolecular interaction between the C-terminal helical region and a central hydrophobic region. Proteomics reveal several Dss1-binding proteins, including all PCI-domain protein complexes. The dynamic fold-back structure regulates Dss1 interactions with the mitotic septins and ATP-citrate lyase.

Highlights

- Dss1 forms a transient and highly dynamic fold-back structure
- Dss1 is associated with multiple protein complexes
- Dss1 is involved in cytokinesis and metabolism

Schenstrøm et al., 2018, Cell Reports *25*, 862–870
October 23, 2018
https://doi.org/10.1016/j.celrep.2018.09.080

CellPress

OPEN ACCESS
CellPress

Cell Reports
Report

Expanded Interactome of the Intrinsically Disordered Protein Dss1

Signe M. Schenstrøm,[1,4] Caio A. Rebula,[1,4] Michael H. Tatham,[2,4] Ruth Hendus-Altenburger,[1] Isabelle Jourdain,[3] Ronald T. Hay,[2] Birthe B. Kragelund,[1] and Rasmus Hartmann-Petersen[1,5,*]

[1]Department of Biology, University of Copenhagen, Ole Maaløes Vej 5, 2200 Copenhagen N, Denmark
[2]Centre for Gene Regulation and Expression, Sir James Black Centre, School of Life Sciences, University of Dundee, Dundee DD1 5EH, UK
[3]College of Life and Environmental Sciences, University of Exeter, Geoffrey Pope Building, Stocker Road, Exeter EX4 4QD, UK
[4]These authors contributed equally
[5]Lead Contact
*Correspondence: rhpetersen@bio.ku.dk
https://doi.org/10.1016/j.celrep.2018.09.080

SUMMARY

Dss1 (also known as Sem1) is a conserved, intrinsically disordered protein with a remarkably broad functional diversity. It is a proteasome subunit but also associates with the BRCA2, RPA, Csn12-Thp1, and TREX-2 complexes. Accordingly, Dss1 functions in protein degradation, DNA repair, transcription, and mRNA export. Here in *Schizosaccharomyces pombe*, we expand its interactome further to include eIF3, the COP9 signalosome, and the mitotic septins. Within its intrinsically disordered ensemble, Dss1 forms a transiently populated C-terminal helix that dynamically interacts with and shields a central binding region. The helix interfered with the interaction to ATP-citrate lyase but was required for septin binding, and in strains lacking Dss1, ATP-citrate lyase solubility was reduced and septin rings were more persistent. Thus, even weak, transient interactions within Dss1 may dynamically rewire its interactome.

INTRODUCTION

Dss1 (Sem1 in budding yeast) is a small and intrinsically disordered eukaryotic protein (IDP) (Dunker et al., 1998; Kragelund et al., 2016; Tompa, 2002; Uversky, 2002; Wright and Dyson, 1999) with a remarkably broad binding specificity. It is a 26S proteasome subunit (Funakoshi et al., 2004; Krogan et al., 2004; Sone et al., 2004) and interacts with the TREX-2 complex (Faza et al., 2009), the BRCA2 DNA repair protein (Yang et al., 2002), the single-strand DNA binding complex RPA (Zhao et al., 2015), and the Csn12-Thp3 complex (Wilmes et al., 2008). A human Dss1 paralog, CSNAP, associates with the COP9 signalosome (CSN) (Rozen et al., 2015).

The flexibility of Dss1 allows it to bind very different surfaces. In the structures of Dss1 in complex with BRCA2 (Yang et al., 2002), the TREX-2 transcription-export complex (Ellisdon et al., 2012), and the 26S proteasome (Dambacher et al., 2016), Dss1 wraps onto its targets in different manners, and even when bound, Dss1 maintains large disordered regions. No universal Dss1 interaction motif has been identified, although several Dss1-interacting proteins contain proteasome, COP9 signalosome, and eukaryotic translation initiation factor 3 (eIF3) (PCI) domains, which function as scaffolds for the formation of protein complexes (Pick et al., 2009).

Genetic studies also suggest a broad functionality: yeast lacking Dss1 display pseudohyphal and temperature-sensitive growth (Jäntti et al., 1999; Jossé et al., 2006; Marston et al., 1999), impaired mRNA export (Faza et al., 2009), and sensitivity to DNA damage (Krogan et al., 2004; Selvanathan et al., 2010). In fission yeast, the growth defect is partially suppressed by expression of other proteasome subunits, suggesting that this phenotype is connected to a destabilization of the 26S proteasome (Jossé et al., 2006; Mannen et al., 2008). Accordingly, budding yeast and *Aspergillus* mutants, lacking the Dss1 ortholog Sem1, are defective in 26S proteasome assembly (Kolog Gulko et al., 2018; Tomko and Hochstrasser, 2014). By a similar chaperone-like function, Dss1 keeps BRCA2 soluble (Yang et al., 2002).

Here, several Dss1 binding partners were found in *Schizosaccharomyces pombe*. Dss1 forms a short C-terminal helix, which folds back and likely limits access to a centrally localized region. The helix inhibits interaction to ATP-citrate lyase (ACLY) and is required for binding to the mitotic septins. The present study shows that the binding specificity of Dss1 is even more diverse than currently appreciated and links Dss1 to additional cellular functions, including metabolism and cell division.

RESULTS

Transient Long-Range Intramolecular Interactions in Dss1

The C terminus of Dss1 has a highly populated α helix (>50%) ranging from F55 to K66 (Figure 1A; Paraskevopoulos et al., 2014), which is independent on the purification method (Figure S1G). We therefore first asked whether Dss1 forms dimers via this structure. However, dilution of Dss1 from 500 to 50 μM did not change the nuclear magnetic resonance (NMR) spectra. To probe for weak interaction, we mixed ^{14}N-Dss1-N71C-MTSL (*S*-(1-oxyl-2,2,5,5-tetramethyl-2,5-dihydro-1H-pyrrol-3-yl)methyl methanesulfonothioate), which places a paramagnetic spin label at the C-terminal of Dss1 (Figures S1A and S1B), with

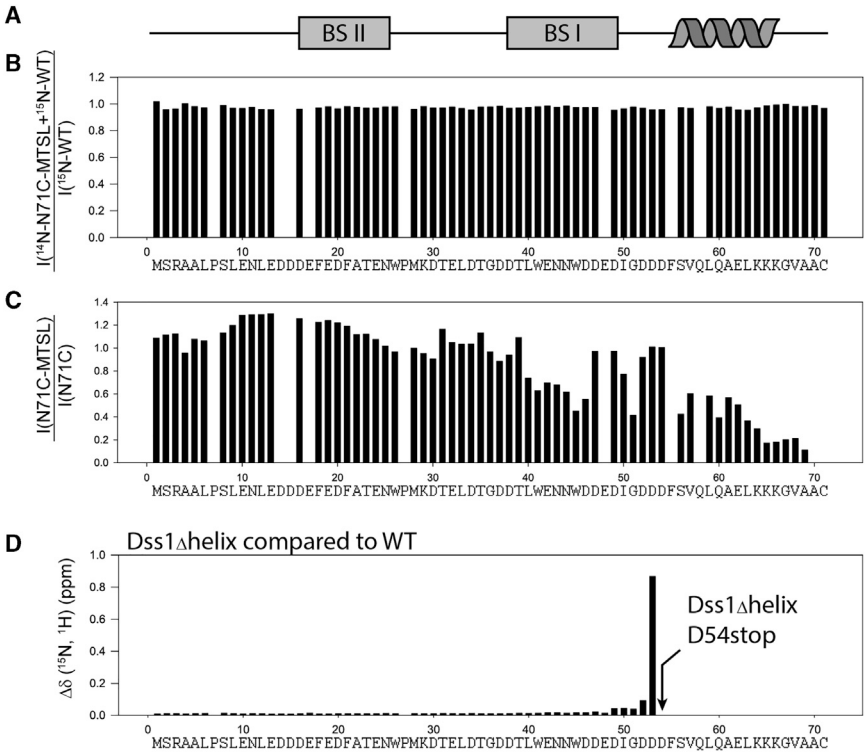

Figure 1. The C-Terminal Region of Dss1 Forms a Dynamic Intramolecular Interaction Limiting Binding Site Access

(A) Dss1 consists of extended structures, including the binding sites BS-I and -II and the transient α helix in the C terminus.

(B) The presence of ^{14}N Dss1-N71C-MTSL (S-(1-oxyl-2,2,5,5-tetramethyl-2,5-dihydro-1H-pyrrol-3-yl)methyl methanesulfonothioate) had no effect on the peak intensities of ^{15}N-Dss1-WT, indicating no inter-molecular interaction.

(C) Intramolecular effect from internal MTSL labeling measured from the effects on the transversal relaxation rate of backbone amide protons of Dss1-N71C-MTSL, resulting in a decrease in the intensity (height) of heteronuclear single quantum coherence (HSQC) peaks of the paramagnetic sample compared to the intensity of the HSQC peaks without the MTSL label.

(D) Truncation of the helix in Dss1Δhelix had no long-range effect on the amide chemical shifts in Dss1.

(E) Different possible conformers of Dss1. The transient α helix in Dss1 forms a dynamic interaction with residues of BS-I, representing a conformational ensemble shielding the BS-I.

See also Figure S1.

^{15}N-Dss1-WT in a 1:1 ratio and recorded NMR paramagnetic relaxation enhancements (PREs), which report on dynamic distances to the label. No transient dimerization was found (Figure 1B). NMR data confirmed that the label did not interfere with the helix population (Figure S1H). However, comparison of the NMR peak intensities of ^{15}N-Dss1-N71C with and without MTSL indicated transient long-range effects from the C-terminal spin label (N71C) to regions >30 residues away. Thus, the C terminus was observed to be close to binding site I (BS-I) as well as to the linker between BS-I and BS-II (Figures 1C and S1C). Deleting the helix from Dss1 (D54stop and Dss1Δhelix) did not affect the amide chemical shifts of residues in BS-I (Figure 1D), suggesting interactions to be mediated by side chains. We propose that the C-terminal helix bends back toward the central binding site of Dss1 and forms dynamic long-range hydrophobic interactions. Consistently, helix formation was not dependent on the presence of the disordered part of Dss1 as a synthetic peptide of the region (D54-G67) was also transiently helical (Figure S1D), just as the CD spectrum of Dss1 was not significantly different compared to the spectral average of the Dss1Δhelix and the helix peptide (Figures S1E and S1F). In support of the fold-back contacts, elevated R_1/R_2 ^{15}N relaxations rate ratios of Dss1 indicated an exchange on a μs–ms timescale for the helix and the interacting region (Figure S1I). Because the PREs, the chemical shifts effects, and the population of the helix are all less than maximal, the helix of Dss1 is not tightly anchored but rather forms a "cloud" that dynamically shields access to the helix itself and to BS-I (Figure 1E). Such equilibrium between open and closed conformations may have consequences for how, and to which extent, the binding sites in Dss1 are available.

Analyses of the Dss1 Interactome

Wild-type Dss1 and Dss1Δhelix were tagged with GFP for affinity purifications. N-terminal fusions were chosen because of the structure (Figure 1E) and since C-terminal tagging of budding yeast Sem1 interferes with some functions (Faza et al., 2009). Full-length fusion protein was incorporated into 26S proteasomes (Figure S2A), localized to the nucleus and cytosol (Figure S2B), and complemented the *dss1*Δ growth defect (Figure S2C). The Dss1Δhelix variant was also efficiently incorporated into 26S proteasomes (Figure S2A) but did not fully complement the *dss1*Δ temperature-dependent growth defect (Figure S2C). The elongated cell morphology (Figure S2D) and accumulation of ubiquitin-protein conjugates (Figure S2E) were also complemented by the full-length GFP-Dss1 fusion protein. However, the elongated cell morphology was not fully suppressed by GFP-Dss1Δhelix

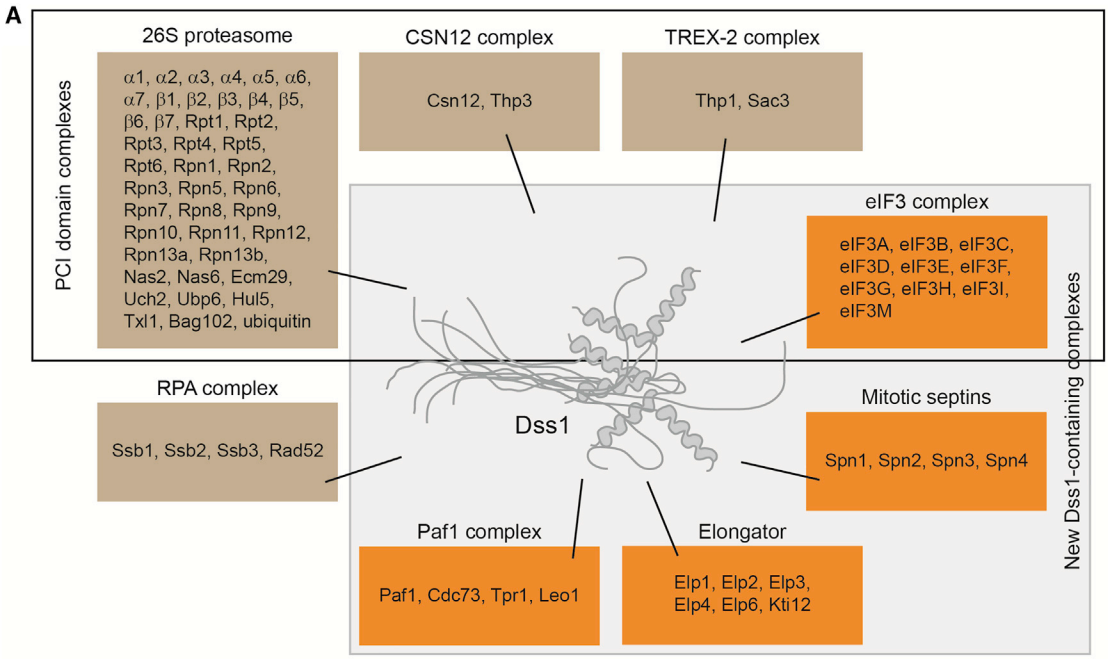

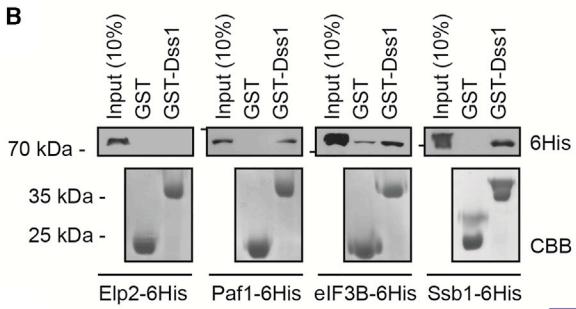

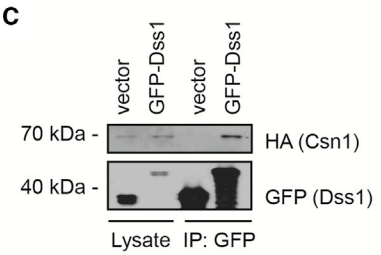

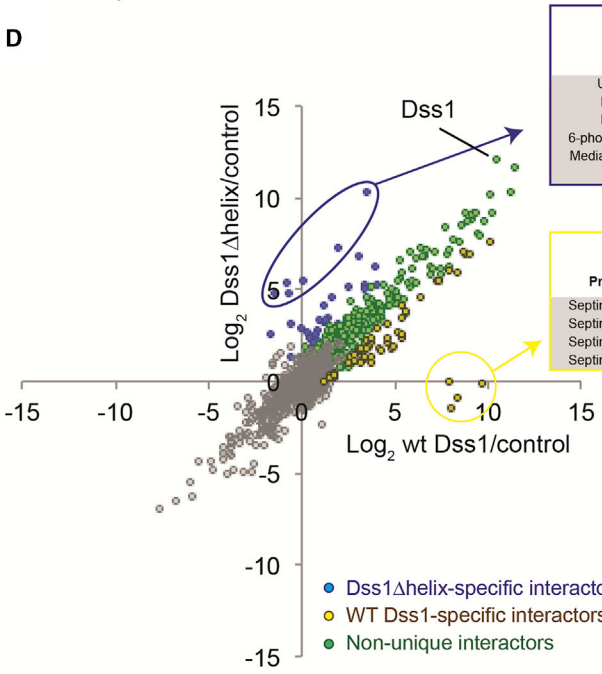

Protein Name	Log_2 WT Dss1/ Control	Log_2 Dss1ΔHelix/ Control	Log_2 Dss1Δhelix/ WT Dss1
Uncharacterized oxidoreductase C1739.08c	3.50	10.36	6.86
Probable ATP-citrate lyase subunit 2, Acl2	-0.85	5.34	6.20
Probable ATP-citrate lyase subunit 1, Acl1	-1.41	4.78	6.19
6-phosphogluconate dehydrogenase, decarboxylating	-0.65	4.82	5.46
Mediator of RNA polymerase II transcription subunit 1	0.13	5.49	5.35
Sorbose reductase, Sou1	1.96	7.25	5.28

Protein Name	Log_2 WT Dss1/ Control	Log_2 Dss1ΔHelix/ Control	Log_2 Dss1Δhelix/ WT Dss1
Septin homolog, Spn3	9.65	-0.07	-9.72
Septin homolog, Spn2	7.99	-1.44	-9.43
Septin homolog, Spn1	8.39	-0.91	-9.30
Septin homolog, Spn4	7.88	0.05	-7.83

(legend on next page)

(Figure S2D). Collectively, this suggests that the N-terminal GFP-tag does not interfere with Dss1 functions.

The GFP-trap system was used to purify proteins from *dss1*Δ cells expressing GFP (control), GFP-Dss1 (wild-type), or GFP-Dss1Δhelix with four replicates of each (Figure S3A). The proteins were identified and quantified by trypsin digestion and liquid chromatography-tandem mass spectrometry (LC-MS/MS) in combination with MaxQuant data analysis. Putative interactors were defined as those proteins that had a GFP-Dss1/GFP intensity ratio >1 and met a 1% false discovery rate (FDR) Student's t test analysis as being significantly different between the two groups. Mass spectrometry data are included in Data S1.

For wild-type Dss1, GFP-Dss1 preparations were enriched in 263 proteins (Figure S3B). They encompass all subunits of the 26S proteasome and several cofactors, all subunits of TREX-2, the CSN12 complex, and RPA (Figure 2A), comprising all known Dss1 interaction partners in yeast (Kragelund et al., 2016). The Dss1 preparations also contained 10 subunits of the PCI-domain complex eIF3, and we found enrichment of subunits of the Paf1 and elongator complexes and all four mitotic septins (Figure 2A).

We then tested a selection of these proteins for interaction with Dss1. Glutathione S-transferase (GST)-Dss1 interacted with Paf1 and Ssb1 and to a lesser extent with eIF3B (Figure 2B). We were unable to detect any interaction to the elongator subunit Elp2.

Intriguingly, the only PCI-domain complex that was not convincingly identified in the mass spectrometry dataset was the CSN. Except for Csn71 (Data S1), no other CSN subunits were significantly enriched in the Dss1 precipitations. Possibly, the CSN in fission yeast is expressed at very low levels (Mundt et al., 1999), or another Dss1-like protein associates with the CSN, as recently shown for the human Dss1 paralog, CSNAP (Rozen et al., 2015). To test this, we precipitated GFP-tagged Dss1 in a strain carrying hemagglutinin (HA)-tagged Csn1. Dss1 did interact weakly with Csn1 (Figure 2C). However, as Nedd8 conjugation to Cul1 was unaffected in the *dss1*Δ strain (Figure S3C), this indicated that Dss1 does not affect the deneddylating function of the CSN, as in human cells lacking CSNAP (Rozen et al., 2015).

The Dss1 Helical Region Restricts Interaction with ACLY

Comparison of the GFP-Dss1 and GFP-Dss1Δhelix interactomes revealed that most interactions (Figures S3D–S3F) occurred independently of the helix (Figure 2D, green points). This agrees with previous reports that most binding to Dss1 is confined to the disordered region (Kragelund et al., 2016), with the Dss1Δhelix complementing most phenotypes of the *dss1*Δ mutant, and with the dynamic character of the fold-back structure. All four mitotic septins showed a clear wild-type-specific binding pattern with little or no evidence for binding to the helix-deficient variant (Figures 2D and S3D–S3F). Conversely, a small group of proteins, including the ATP-citrate lyase (ACLY) subunits Acl1 and Acl2, showed binding preference for the Dss1Δhelix variant over wild-type Dss1 (Figure 2D). This implies that the helical region has a negative effect on the association of these proteins.

Confirmatively, two proteins of ~60 kDa co-precipitated with GFP-Dss1Δhelix (Figures 3A and S3A). Mass spectrometry identified them as Acl1 (67.2 kDa; sequence coverage 55%) and Acl2 (53.9 kDa; sequence coverage 54%). Unlike in humans where ACLY is a homotetramer (Chypre et al., 2012), fission yeast ACLY is encoded by *acl1* that resembles the C-terminal part of human ACLY and *acl2* that resembles the N-terminal part of human ACLY. The ACLY binding site was mapped by precipitation experiments. ACLY was primarily associated with Dss1 when the helix was removed (Figure 3B), and the interaction was lost upon further mutation of the disordered region (Figure 3B). The interaction between Dss1Δhelix and ACLY was also evident in a wild-type background, although to a lesser degree (Figure 3C). In an *acl1*Δ strain, neither subunit was co-precipitated, and in an *acl2*Δ strain, only Acl1 was co-precipitated (Figure 3C), indicating that association of ACLY and Dss1 primarily occurs via the Acl1 subunit and this interaction is inhibited by the dynamic fold-back structure.

As Dss1 promotes BRCA2 solubility (Yang et al., 2002), we tested whether this was also the case for ACLY in wild-type, *dss1*Δhelix, and *dss1*Δ cells. Dss1 and Dss1Δhelix were both soluble proteins. However, more Acl1 was insoluble in the *dss1*Δ cells (Figures 3D and 3E) than in *dss1*Δhelix cells, suggesting that Dss1 binding facilitates ACLY solubility.

Because ACLY converts cytosolic citrate into acetyl-coenzyme A (CoA) (Chypre et al., 2012), which is required for fatty acids synthesis, we analyzed the lipid content in wild-type, *acl1*Δ, *acl2*Δ, and *dss1*Δ strains. As a control, we included a *cut6-621* strain that is defective in acetyl-CoA carboxylase, which is required for fatty acid biosynthesis (Saitoh et al., 1996). The lipid droplets appeared unaffected in the ACLY mutants (Figure S4A) but strongly reduced in *dss1*Δ cells and the *cut6-621* control, suggesting that ACLY does not contribute much acetyl-CoA for fatty acid biosynthesis and that the reduced amount of lipids in the *dss1*Δ strain is independent of ACLY. Accordingly, the *acl1*Δ and *acl2*Δ strains did not display any

Figure 2. Quantitative Mass Spectrometry and Dss1 Binding Partners

(A) Dss1 binding partners were clustered into known protein complexes. The PCI-domain-containing complexes are framed (transparent). All data are included in Data S1.

(B) Extracts from wild-type strains, expressing the indicated 6His-tagged proteins, were used for co-precipitation with GST-Dss1 and GST. The precipitated material was analyzed by blotting for the 6His tag. Equal loading was checked by staining with Coomassie brilliant blue (CBB).

(C) Cells with HA-tagged Csn1 and expressing either GFP or GFP-Dss1 were used for immunoprecipitation (IP) using GFP-trap. The precipitated material was analyzed by blotting for the HA-tag or GFP (Dss1).

(D) Plot of the fold change in GFP-Dss1 versus GFP (x axis) versus the fold change in GFP-Dss1Δhelix versus GFP (y axis). Proteins marked in green were unaffected by deletion of the C-terminal region. Proteins marked in blue were more associated with Dss1Δhelix, and proteins marked in yellow were less associated with Dss1Δhelix.

See also Figures S2 and S3.

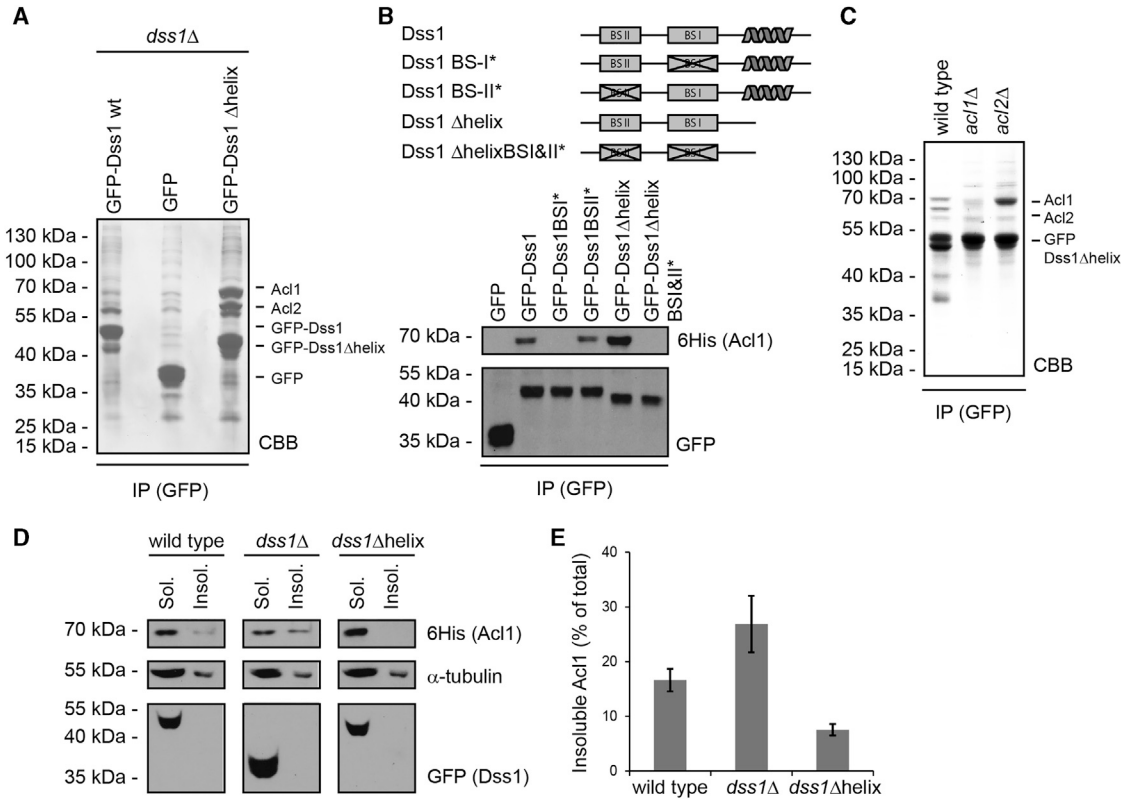

Figure 3. The C-Terminal Region Blocks Dss1 Binding to ACLY

(A) *dss1*Δ transformed to produce GFP, GFP-Dss1, and GFP-Dss1Δhelix was used for IP using GFP-trap. The precipitated material was analyzed by SDS-PAGE and CBB staining. The identity of Acl1 and Acl2 was determined by mass spectrometry.

(B) *dss1*Δ cells, expressing the Dss1 variants (upper panel), were used for IP using GFP-trap. BS-I* and BS-II* indicate point mutations in the BS-I and BS-II binding sites (BS-I*: L40A/W41A/W45A; BS-II*: F18A/F21A/W26A). The precipitated material was analyzed by blotting.

(C) The indicated strains expressing GFP-Dss1Δhelix were used for IP using GFP-trap. The precipitated material was analyzed by SDS-PAGE and CBB staining.

(D) The solubility of 6His-tagged Acl1 was determined by centrifugation of whole-cell extracts and blotting.

(E) Blots as shown in (D) were quantified by densitometry and presented as percent of total (sol. + insol.). The error bars indicate the SEM (n = 3).

See also Figure S4.

obvious growth defects (Figure S4B). The redundancy of ACLY may be caused by the cytosolic enzyme acetyl-coA synthetase, Acs1.

The Dss1 C-Terminal Helical Region Is Required for Interaction with Mitotic Septins

The mitotic septins (Spn1–4) only bind to wild-type Dss1 and not to the truncated Dss1Δhelix (Figure 2D). We found that HA-tagged Spn3 and Spn4 precipitate with Dss1 (Figure 4A). In agreement with the proteomics analyses, further co-precipitation experiments revealed that the helical region in Dss1 was required for septin interaction (Figure 4B).

As with ACLY, septin solubility correlated with binding specificity for the Dss1 variants. Septin solubility was greater in wild-type cells than in the *dss1*Δ strain and appeared to depend on the C-terminal region (Figures 4C and 4D). In *dss1*Δ, Spn3-GFP correctly localized at the cell equator as a single or double ring. There was no apparent reduction in signal intensity compared to that in wild-type cells (Figure 4E). This suggests that Dss1 functions downstream of septin ring formation. A closer observation of Spn3-GFP by time-lapse microscopy revealed that many septin rings were more persistent in the absence of Dss1 (Figure 4F; average time of septins at cell equator in the wild-type [WT] = 46.1 ± 0.5 min, n = 126; *dss1*Δ = 55.9 ± 2.1, n = 94; $p < 0.0001$). We conclude that Dss1 may affect septin maintenance, rather than recruitment, during cytokinesis.

DISCUSSION

Previously, Dss1 has been suggested as a component of the eIF3 complex (Pick et al., 2009). Our data support this notion. The *S. pombe* eIF3 subunits, eIF3a, eIF3c, and eIF3m, contain PCI domains and all associated with Dss1. CSN was the only PCI domain protein complex that was not found in our proteomics analyses. However, Dss1 and Csn1 co-precipitated, so perhaps in fission yeast, which is without CSNAP, Dss1 may fulfill the function of CSNAP in the CSN, which neither in human cells (Rozen et al., 2015) nor in fission yeast involves the deneddylating activity of the CSN.

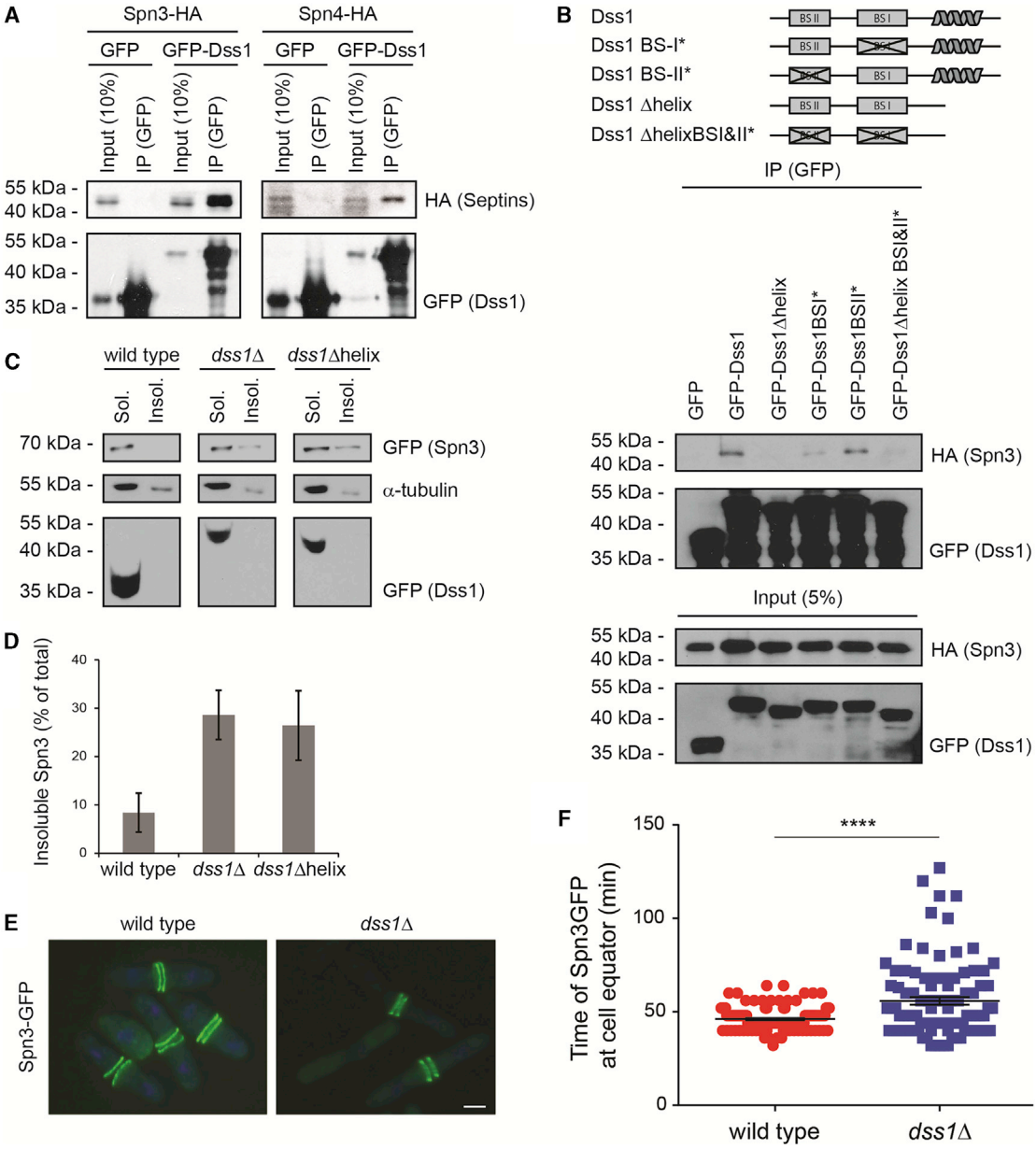

Figure 4. The C-Terminal Region Is Required for Dss1 Interaction with Mitotic Septins

(A) Cells with HA-tagged Spn3 or Spn4 and expressing either GFP or GFP-Dss1 were used for IP using GFP-trap. The precipitated material was analyzed by blotting for the HA-tag or GFP.

(B) Cells with HA-tagged Spn3 and expressing either GFP or GFP-Dss1 variants (upper panel) were used for IP using GFP-trap. BS-I* and BS-II* indicate point mutations in the BS-I and BS-II binding sites (BS-I*: L40A/W41A/W45A; BS-II*: F18A/F21A/W26A). The precipitated material was analyzed by SDS-PAGE and blotting for the HA-tag or GFP.

(C) The solubility of GFP-tagged Spn3 was determined by centrifugation of whole-cell extracts and blotting.

(D) Blots as shown in (C) were quantified by densitometry and presented as percent of total (sol. + insol.). The error bars indicate the SEM (n = 3).

(E) The septum ring of wild-type and *dss1*Δ cells was observed by fluorescence microscopy using Spn3-GFP as a marker. Scale bar represents 5 μm.

(F) Wild-type and *dss1*Δ cells expressing Spn3-GFP were observed at 27°C over time by fluorescence microscopy, and the duration of the GFP signal was quantified. Each circle or square represents the timing in 1 cell. Black bars represent the average and SEM; n > 94 cells; 2 experiments. Unpaired two-tailed t test; ****$p < 0.0001$.

Free Dss1 is disordered but attains structure upon binding to BRCA2, TREX-2, and the 26S proteasome (Kragelund et al., 2016). The structure of Dss1 in each of these complexes is different, and large parts of Dss1 remain disordered. This may also be the case for the Dss1-binding proteins identified here.

Dss1 interacts with BRCA2 (Yang et al., 2002), keeping BRCA2 soluble and facilitating dissociation of RPA from DNA, allowing access for BRCA2 (Zhao et al., 2015). *S. pombe* has no BRCA2 ortholog, but the Dss1-RPA interaction is conserved. In addition, Dss1 associates with Rad52, which stimulates strand exchange. In agreement, yeast Dss1 localizes to double-strand breaks and promotes DNA repair (Krogan et al., 2004; Selvanathan et al., 2010), suggesting that Dss1 stimulates DNA dissociation of RPA also in yeast.

It is likely that many of the interactions are not direct. It is possible, for instance, that the TREX-2 complex bridges the interaction with elongator and the Paf1 complex because budding yeast TREX-2 mutants display synthetic phenotypes with components in the Paf1 and elongator complexes (Collins et al., 2007; Wilmes et al., 2008). Accordingly, mutants in the Paf1 complex are also epistatic with mutants in elongator (Collins et al., 2007; Laribee et al., 2005). Along the same line, eIF3 has previously been found to associate with the 26S proteasome (Sha et al., 2009), and because Dss1 binds ubiquitin, some interactions might even be interceded by ubiquitin.

The Dss1 C-terminal helix can fold back and form a transient interaction with BS-I. Helix formation was independent of intramolecular interaction and inherent to the amino acid sequence. Access to BS-I as well as the helix itself may be controlled by an open-closed equilibrium through a population shift mechanism (Vallée-Bélisle et al., 2009) as seen with other IDPs. Helix propensity has, for instance, been linked to ligand binding (Borcherds et al., 2014; Ješmantavičius et al., 2014), and a change in the structural ensemble can also be introduced by posttranslational modifications (Bah and Forman-Kay, 2016; Bui and Gsponer, 2014). We therefore propose that even the weak, transient interactions, formed between the helix and the central binding site, can regulate the Dss1 interactome.

Contrary to the situation with ACLY, we found that the C-terminal helical region of Dss1 was required for interaction with the septins. *S. pombe* has four mitotic septins that assemble into hetero-oligomeric complexes in interphase (An et al., 2004). During mitosis, the septins concentrate at the medial region of the cell to form ring-shaped structures that are binding scaffolds for other proteins. Previous studies have tied Dss1 to the Spt-Ada-Gcn5-acetyltransferase (SAGA) complex (García-Oliver et al., 2013), which regulates septin ring assembly via transcriptional activation of *mid2*$^{+}$ (Lei et al., 2014). We did not observe any defects in septin ring formation in the *dss1*-null mutant, but we cannot rule out that the role of Dss1 in transcription contributes to the *dss1*Δ septation problems.

The present study shows how the flexibility of an IDP allows it to accommodate binding to a plethora of protein complexes and suggests that intramolecular transient structures and their relatively weak interactions may be sufficient to rewire interaction networks. How this is timed and controlled should be the focus of future work.

EXPERIMENTAL PROCEDURES

Yeast Strains and Plasmids

Strains were kindly provided by Dr. Colin Gordon, Dr. Michael Seeger, Dr. Mitsuhiro Yanagida, and Dr. Kathleen L. Gould. All strains (Table S1; all strains used for this study) and procedures used in this work are listed in the Supplemental Information.

Protein Purification and Proteomic Analyses

Protocols for protein purification, NMR analyses, and proteomics are provided in the Supplemental Information. For co-precipitation experiments, GFP-, GFP-Dss1-, and GFP-Dss1Δhelix-expressing cultures of 2 L were set up in quadruplicates and grown at 29°C to mid-exponential phase. The cells were then harvested by centrifugation (3,000 *g*; 10 min) and lysed in Buffer C (25 mM Tris/HCl [pH 7.4], 50 mM NaCl, 2 mM $MgCl_2$, 2 mM ATP, 10% glycerol, 0.1% Triton X-100, 1 mM PMSF, and Complete protease inhibitors; Roche) at 4°C using glass beads and a FastPrep machine (Thermo Scientific). Lysates were cleared (13,000 *g*; 30 min) and tumbled with 30 μL GFP-trap (Chromotek) beads for 4 hr at 4°C. Beads were washed in 4 × 1 mL Buffer C by centrifugation (3,000 *g*; 30 s) and finally resuspended into 30 μL SDS sample buffer. Identification of Acl1 and Acl2 by MALDI MS/MS was performed by Alphalyse (Denmark). Co-precipitations with GST-tagged proteins were performed as in Paraskevopoulos et al. (2014).

Microscopy

We used an inverted Zeiss microscope and Axiovision software, a Plan Apo 100× oil objective, numerical aperture (NA) = 1.4, and a CoolSnap HQ camera. Detailed protocols are in the Supplemental Information.

Nuclear Magnetic Resonance

Detailed protocols are in the Supplemental Information.

Statistics

For the mass spectrometry, proteins were defined as statistically differing between groups using the Perseus unpaired two-sample Student's t test truncated by 1% permutation-based FDR using an S0 value of 0.1. Complex enrichment analysis was performed in Perseus using the Fisher's exact test using the different sub-categories of the data as comparison with the whole set of 1,005 proteins. For western blots, statistical analyses were performed in MS Excel. The results are presented as average and SEM. For time-lapse imaging, statistical analysis was performed with Prism using an unpaired two-tailed t test. The results are presented as average and SEM.

DATA AND SOFTWARE AVAILABILITY

The accession number for the chemical shifts reported in this paper is Biological Magnetic Resonance Data Bank: 27618.

SUPPLEMENTAL INFORMATION

Supplemental Information includes Supplemental Experimental Procedures, four figures, one table, and one data file and can be found with this article online at https://doi.org/10.1016/j.celrep.2018.09.080.

ACKNOWLEDGMENTS

The authors thank Dr. Colin Gordon, Dr. Michael Seeger, Dr. Dieter A. Wolf, Dr. Kathleen L. Gould, and Dr. Mitsuhiro Yanagida for materials; Mrs. Anne-Marie Lauridsen, Mrs. Signe A. Sjørup, Ms. Rikke Brandstrup, Ms. Sara M. Ambjørn, Dr. Ida S.B. Larsen, Dr. Franziska Kriegenburg, Dr. Heike Rösner, and Dr. Helen Dawe for excellent technical support; and Dr. K.B. Hendil for comments on the manuscript. R.H.-P. is supported by the Lundbeck Foundation, The Danish Cancer Society, the Novo Nordisk Foundation, the A.P. Møller Foundation, and the Danish Council for Independent Research (Natural Sciences). B.B.K. is supported by the Danish Council for Independent Research (Natural Sciences; 12-128803), the Novo Nordisk Foundation, the Villum Foundation, and the Carlsberg Foundation; M.H.T. by CRUK; and C.A.R. by the Coordination for the Improvement of Higher Level Education Personnel (CAPES) from the Brazilian Ministry of Education. This article is based upon work from COST Action (PROTEOSTASIS BM1307; European Cooperation in Science and Technology).

AUTHOR CONTRIBUTIONS

S.M.S., C.A.R., M.H.T., R.H.-A., and I.J. conducted the experiments. S.M.S., M.H.T., R.H.-A., R.T.H., I.J., B.B.K., and R.H.-P. designed the experiments and analyzed the data. S.M.S., B.B.K., and R.H.-P. wrote the paper.

DECLARATION OF INTERESTS

The authors declare no competing interests.

Received: January 3, 2018
Revised: April 24, 2018
Accepted: September 25, 2018
Published: October 23, 2018

REFERENCES

An, H., Morrell, J.L., Jennings, J.L., Link, A.J., and Gould, K.L. (2004). Requirements of fission yeast septins for complex formation, localization, and function. Mol. Biol. Cell *15*, 5551–5564.

Bah, A., and Forman-Kay, J.D. (2016). Modulation of intrinsically disordered protein function by post-translational modifications. J. Biol. Chem. *291*, 6696–6705.

Borcherds, W., Theillet, F.X., Katzer, A., Finzel, A., Mishall, K.M., Powell, A.T., Wu, H., Manieri, W., Dieterich, C., Selenko, P., et al. (2014). Disorder and residual helicity alter p53-Mdm2 binding affinity and signaling in cells. Nat. Chem. Biol. *10*, 1000–1002.

Bui, J.M., and Gsponer, J. (2014). Phosphorylation of an intrinsically disordered segment in Ets1 shifts conformational sampling toward binding-competent substates. Structure *22*, 1196–1203.

Chypre, M., Zaidi, N., and Smans, K. (2012). ATP-citrate lyase: a mini-review. Biochem. Biophys. Res. Commun. *422*, 1–4.

Collins, S.R., Miller, K.M., Maas, N.L., Roguev, A., Fillingham, J., Chu, C.S., Schuldiner, M., Gebbia, M., Recht, J., Shales, M., et al. (2007). Functional dissection of protein complexes involved in yeast chromosome biology using a genetic interaction map. Nature *446*, 806–810.

Dambacher, C.M., Worden, E.J., Herzik, M.A., Martin, A., and Lander, G.C. (2016). Atomic structure of the 26S proteasome lid reveals the mechanism of deubiquitinase inhibition. eLife *5*, e13027.

Dunker, A.K., Garner, E., Guilliot, S., Romero, P., Albrecht, K., Hart, J., Obradovic, Z., Kissinger, C., and Villafranca, J.E. (1998). Protein disorder and the evolution of molecular recognition: theory, predictions and observations. Pac. Symp. Biocomput., 473–484.

Ellisdon, A.M., Dimitrova, L., Hurt, E., and Stewart, M. (2012). Structural basis for the assembly and nucleic acid binding of the TREX-2 transcription-export complex. Nat. Struct. Mol. Biol. *19*, 328–336.

Faza, M.B., Kemmler, S., Jimeno, S., González-Aguilera, C., Aguilera, A., Hurt, E., and Panse, V.G. (2009). Sem1 is a functional component of the nuclear pore complex-associated messenger RNA export machinery. J. Cell Biol. *184*, 833–846.

Funakoshi, M., Li, X., Velichutina, I., Hochstrasser, M., and Kobayashi, H. (2004). Sem1, the yeast ortholog of a human BRCA2-binding protein, is a component of the proteasome regulatory particle that enhances proteasome stability. J. Cell Sci. *117*, 6447–6454.

García-Oliver, E., Pascual-García, P., García-Molinero, V., Lenstra, T.L., Holstege, F.C., and Rodríguez-Navarro, S. (2013). A novel role for Sem1 and TREX-2 in transcription involves their impact on recruitment and H2B deubiquitylation activity of SAGA. Nucleic Acids Res. *41*, 5655–5668.

Ješmantavičius, V., Dogan, J., Jemth, P., Teilum, K., and Kjaergaard, M. (2014). Helical propensity in an intrinsically disordered protein accelerates ligand binding. Angew. Chem. Int. Ed. Engl. *53*, 1548–1551.

Jäntti, J., Lahdenranta, J., Olkkonen, V.M., Söderlund, H., and Keränen, S. (1999). SEM1, a homologue of the split hand/split foot malformation candidate gene Dss1, regulates exocytosis and pseudohyphal differentiation in yeast. Proc. Natl. Acad. Sci. USA *96*, 909–914.

Jossé, L., Harley, M.E., Pires, I.M., and Hughes, D.A. (2006). Fission yeast Dss1 associates with the proteasome and is required for efficient ubiquitin-dependent proteolysis. Biochem. J. *393*, 303–309.

Kolog Gulko, M., Heinrich, G., Gross, C., Popova, B., Valerius, O., Neumann, P., Ficner, R., and Braus, G.H. (2018). Sem1 links proteasome stability and specificity to multicellular development. PLoS Genet. *14*, e1007141.

Kragelund, B.B., Schenstrøm, S.M., Rebula, C.A., Panse, V.G., and Hartmann-Petersen, R. (2016). DSS1/Sem1, a multifunctional and intrinsically disordered protein. Trends Biochem. Sci. *41*, 446–459.

Krogan, N.J., Lam, M.H., Fillingham, J., Keogh, M.C., Gebbia, M., Li, J., Datta, N., Cagney, G., Buratowski, S., Emili, A., and Greenblatt, J.F. (2004). Proteasome involvement in the repair of DNA double-strand breaks. Mol. Cell *16*, 1027–1034.

Laribee, R.N., Krogan, N.J., Xiao, T., Shibata, Y., Hughes, T.R., Greenblatt, J.F., and Strahl, B.D. (2005). BUR kinase selectively regulates H3 K4 trimethylation and H2B ubiquitylation through recruitment of the PAF elongation complex. Curr. Biol. *15*, 1487–1493.

Lei, B., Zhou, N., Guo, Y., Zhao, W., Tan, Y.W., Yu, Y., and Lu, H. (2014). Septin ring assembly is regulated by Spt20, a structural subunit of the SAGA complex. J. Cell Sci. *127*, 4024–4036.

Mannen, T., Andoh, T., and Tani, T. (2008). Dss1 associating with the proteasome functions in selective nuclear mRNA export in yeast. Biochem. Biophys. Res. Commun. *365*, 664–671.

Marston, N.J., Richards, W.J., Hughes, D., Bertwistle, D., Marshall, C.J., and Ashworth, A. (1999). Interaction between the product of the breast cancer susceptibility gene BRCA2 and DSS1, a protein functionally conserved from yeast to mammals. Mol. Cell. Biol. *19*, 4633–4642.

Mundt, K.E., Porte, J., Murray, J.M., Brikos, C., Christensen, P.U., Caspari, T., Hagan, I.M., Millar, J.B., Simanis, V., Hofmann, K., and Carr, A.M. (1999). The COP9/signalosome complex is conserved in fission yeast and has a role in S phase. Curr. Biol. *9*, 1427–1430.

Paraskevopoulos, K., Kriegenburg, F., Tatham, M.H., Rösner, H.I., Medina, B., Larsen, I.B., Brandstrup, R., Hardwick, K.G., Hay, R.T., Kragelund, B.B., et al. (2014). Dss1 is a 26S proteasome ubiquitin receptor. Mol. Cell *56*, 453–461.

Pick, E., Hofmann, K., and Glickman, M.H. (2009). PCI complexes: beyond the proteasome, CSN, and eIF3 Troika. Mol. Cell *35*, 260–264.

Rozen, S., Füzesi-Levi, M.G., Ben-Nissan, G., Mizrachi, L., Gabashvili, A., Levin, Y., Ben-Dor, S., Eisenstein, M., and Sharon, M. (2015). CSNAP is a stoichiometric subunit of the COP9 signalosome. Cell Rep. *13*, 585–598.

Saitoh, S., Takahashi, K., Nabeshima, K., Yamashita, Y., Nakaseko, Y., Hirata, A., and Yanagida, M. (1996). Aberrant mitosis in fission yeast mutants defective in fatty acid synthetase and acetyl CoA carboxylase. J. Cell Biol. *134*, 949–961.

Selvanathan, S.P., Thakurta, A.G., Dhakshnamoorthy, J., Zhou, M., Veenstra, T.D., and Dhar, R. (2010). Schizosaccharomyces pombe Dss1p is a DNA damage checkpoint protein that recruits Rad24p, Cdc25p, and Rae1p to DNA double-strand breaks. J. Biol. Chem. *285*, 14122–14133.

Sha, Z., Brill, L.M., Cabrera, R., Kleifeld, O., Scheliga, J.S., Glickman, M.H., Chang, E.C., and Wolf, D.A. (2009). The eIF3 interactome reveals the translasome, a supercomplex linking protein synthesis and degradation machineries. Mol. Cell *36*, 141–152.

Sone, T., Saeki, Y., Toh-e, A., and Yokosawa, H. (2004). Sem1p is a novel subunit of the 26 S proteasome from Saccharomyces cerevisiae. J. Biol. Chem. *279*, 28807–28816.

Tomko, R.J., Jr., and Hochstrasser, M. (2014). The intrinsically disordered Sem1 protein functions as a molecular tether during proteasome lid biogenesis. Mol. Cell *53*, 433–443.

Tompa, P. (2002). Intrinsically unstructured proteins. Trends Biochem. Sci. *27*, 527–533.

Uversky, V.N. (2002). Natively unfolded proteins: a point where biology waits for physics. Protein Sci. *11*, 739–756.

Vallée-Bélisle, A., Ricci, F., and Plaxco, K.W. (2009). Thermodynamic basis for the optimization of binding-induced biomolecular switches and structure-switching biosensors. Proc. Natl. Acad. Sci. USA *106*, 13802–13807.

Wilmes, G.M., Bergkessel, M., Bandyopadhyay, S., Shales, M., Braberg, H., Cagney, G., Collins, S.R., Whitworth, G.B., Kress, T.L., Weissman, J.S., et al. (2008). A genetic interaction map of RNA-processing factors reveals links between Sem1/Dss1-containing complexes and mRNA export and splicing. Mol. Cell *32*, 735–746.

Wright, P.E., and Dyson, H.J. (1999). Intrinsically unstructured proteins: re-assessing the protein structure-function paradigm. J. Mol. Biol. *293*, 321–331.

Yang, H., Jeffrey, P.D., Miller, J., Kinnucan, E., Sun, Y., Thoma, N.H., Zheng, N., Chen, P.L., Lee, W.H., and Pavletich, N.P. (2002). BRCA2 function in DNA binding and recombination from a BRCA2-DSS1-ssDNA structure. Science *297*, 1837–1848.

Zhao, W., Vaithiyalingam, S., San Filippo, J., Maranon, D.G., Jimenez-Sainz, J., Fontenay, G.V., Kwon, Y., Leung, S.G., Lu, L., Jensen, R.B., et al. (2015). Promotion of BRCA2-dependent homologous recombination by DSS1 via RPA targeting and DNA mimicry. Mol. Cell *59*, 176–187.